euspen's 23rd International Conference & Exhibition, Copenhagen, DK, June 2023
www.euspen.eu

Concentric jet for confined mask-less anodic dissolution and oxidation of aluminium

André Martin[1,*], Susanne Quitzke[1], Roy Morgenstern[2], Andreas Schubert[1,3], Thomas Lampke[2]

[1] Chemnitz University of Technology, Institute for Machine Tools and Production Processes, Professorship Micromanufacturing Technology, Reichenhainer Str. 70, 09126 Chemnitz, Germany
[2] Chemnitz University of Technology, Institute of Materials Science and Engineering, Materials and Surface Engineering, Erfenschlager Str. 73, 09125 Chemnitz, Germany
[3] Fraunhofer Institute for Machine Tools and Forming Technology, Reichenhainer Str. 88, 09126 Chemnitz, Germany

*email address of the submitting author: andre.martin@mb.tu-chemnitz.de

Abstract
Anodic oxide layers are established for wear and corrosion protection of surfaces of aluminium parts and for decoration purposes. Usually, anodizing is carried out in large scale on the whole part surface or locally by masking through immersion in an electrolytic bath. Applying a free jet of electrolyte offers laterally confined anodizing without extensive efforts for masking and enables local functionalization without undesired influence on the surrounding surfaces in a resource- and energy-efficient process. However, the high ohmic resistance of anodic oxides leads to a wide distribution of the current density hindering laterally confined anodizing. More sharp-contoured anodic oxides are aspired through dilution of the electrolyte film flowing off laterally from the aluminium surface.
For this purpose, a concentric arrangement of an electrolyte jet surrounded by a jet of deionized water was realized. Investigations on the distribution of electric current density were carried out by electrochemical machining experiments (Jet-ECM). The application of an actively anodic dissolving electrolyte of NaCl indicates the widening of the current density distribution in terms of pitting corrosion. Compared to the free electrolyte jet surrounded by atmospheric air, a wider current density distribution was detected when applying a concentric jet of deionized water. But the shape of the dissolved cavities was not widened, which indicates only low current density values on the surrounding surface. Verification experiments on anodization confirm the comparably strong localization of anodic oxides with concentric jet and an increase in thickness compared to the results with free electrolytic jet. It was found that this is mainly because of the high ohmic resistance of the anodic oxide formed on the surrounding surface and its increasing resistance at farther lateral distance from the jet due to stronger electrolyte dilution.

Keywords: concentric jet, locally confined anodic oxide, mask-less anodizing of aluminium, free electrolytic jet, Jet-ECM

1. Introduction

Anodic oxidation is an established technique to create protective layers on parts made of aluminium alloys against extensive corrosive attacks or from abrasive wear [1]. Colouring of the porous anodic oxides is often used for colour-scaled markings or for decorative issues [2]. Anodizing of the whole part surfaces, as usually carried out in immersion-based processes, requires extensive consumption of electric energy with quadratic increase at linear increase of the part dimensions.

Localization of the anodization process by lateral confinement to the relevant surfaces not only offers the possibility to significantly reduce electric energy consumption but also enables avoiding unwanted influences on the surrounding surfaces, e.g. where the characteristic intrinsic stresses in case of mechanically loaded parts [3,4] or oxides on blank surfaces in case of electrical contacts might have negative effects and need to be avoided. Localization is yet realized by masking the surrounding surfaces, which needs to be applied before anodization and removed afterwards. Efforts for the application and the removal of the masking increase extensively, when locally confined, contoured functionalization is aspired. Adhesive tapes containing viscous electrolytic media can be applied to specifically address the aspired contours [5]. But the restricted mass transport through the viscous media only offers low growth rates and lower oxide thickness in comparison to conventional processes.

As an alternative, brush anodization is applied to repair defects on large components such as aircraft parts for local restoration of the corrosion and wear protection [6,7,8]. Another possibility for contoured surface anodization is the application of capillaries [9,10]. The latter offers laterally sharp confinements. However, lateral sealing of the capillary needs to be assured, which only works on planar surfaces and reduces the application and its flexibility. Predefined capillary diameters and brush widths reduce the lateral flexibility and vertical positioning must be carried out very precisely to assure predefined results.

As an alternative, the application of a free electrolyte jet represents a promising technique with high flexibility to locally apply electrolytic solution thus confining the electric current density in the near of the impinging jet without masking. Previous studies on jet-electrochemical machining [11] and jet-based anodization [12] have shown the possibility to transfer this technology from electrochemical dissolution to anodization with locally confined results. The results indicate that resource- and energy-efficient anodization is possible with reduced voltage and working gap that offered decreased electric energy consumption and improved localization [12,13]. Hence, localized functionalization with controllable result regarding anodic oxide thickness is possible and surrounding surfaces are hardly influenced at short processing times.

However, increasing the anodization time results in higher ohmic resistance of the anodic oxide and leads to widening of the current density distribution. Hence, localization is reduced, and laterally well-defined confinement of the anodic oxides is

hardly controllable, when massive oxides requiring long anodization times are aspired. For this purpose, dilution of the electrolyte film flowing off laterally over the part's surface after being ejected from the nozzle is investigated in this study. The aim is to reduce the effect of the increasing electric resistance of the anodic oxide layer, which results in a wide distribution of current density and, hence, in a widening of oxide formation and reduced thickness in the centre of the impinging electrolyte jet.

In anodization, the electrolyte can be considered as electrical resistance connected in series to the resistance of the anodic oxide. Since the electrolyte only has a low resistance compared to the oxide, electric charge is transported over large radial distances of the workpiece surface. Hence, dilution of the electrolyte film should enable reducing this effect and increasing the localisation of the electric charge exchange to the near of the impinging electrolyte jet.

2. Experimental

To analyse the influence of the electrolyte film dilution on the current density distribution and the material dissolution, an established arrangement was used. Figure 1 shows the principle arrangement of the electrolyte nozzle with concentric nozzle for the supply of compressed air and deionized water (dionate).

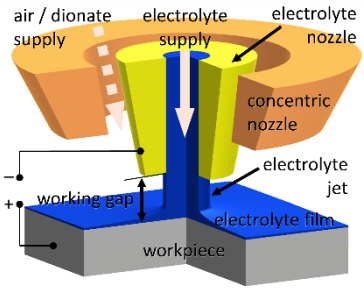

Figure 1. Principle of the concentric arrangement using free electrolyte jet in compressed, atmospheric air and concentric jet of dionate

The electrolyte nozzle (yellow) is positioned at a predefined working distance perpendicularly from the workpiece surface (grey). Supply of electrolyte (blue) with a flow rate of approximately 20 m/s leads to the formation of a free jet, when compressed, atmospheric air is supplied through the concentric nozzle (orange). Supply of dionate through the concentric nozzle offers the possibility for dilution of the electrolyte film with negligible influence on the electrolyte jet.

The experimental parameters for free electrolyte jet (Jet-ECM) and concentric jet of dionate charted in Table 1 were chosen according to previous studies [11].

Table 1 Parameters for Jet-ECM removal experiments

parameter	value
Voltage	60 V
Sample material	Stainless steel 1.4301
Removal time	1 s
Working gap	100 µm
Electrolyte nozzle diameter	100 µm
Dionate nozzle diameter	1000 µm
Electrolyte solution	100 g/l NaCl, aqueous
Electrolyte conductivity	110 mS/cm
Electrolyte supply rate	10 ml/min

An actively anodic dissolving electrolyte of NaCl was chosen to analyse the current density distribution from active dissolution at low current density values by means of stray removal effects. For this purpose, local machining experiments without nozzle movement were arranged on the part's surface.

Anodization experiments with free electrolyte jet and with concentric dionate jet were carried out with the parameters charted in Table 2.

Table 2 Parameters for jet anodization experiments

parameter	value
Voltage	40 V
Sample material	Aluminium EN AW-7075 T6
Anodization time	10 min
Working gap	100 µm
Electrolyte nozzle diameter	100 µm
Dionate nozzle diameter	1000 µm
Electrolyte solution	6,1 g/l oxalic acid
Electrolyte conductivity	60 mS/cm
Electrolyte supply rate	10 ml/min

A voltage with an amplitude of 40 V was applied using rectangular pulses with a frequency of 200 Hz. Considering the duty cycle of 50 % over a total processing time of 20 min resulted in an effective anodization time of 10 min.

3. Results of Jet-ECM removal experiments

The measured electric current values with and without concentric dionate jet are presented in figure 2.

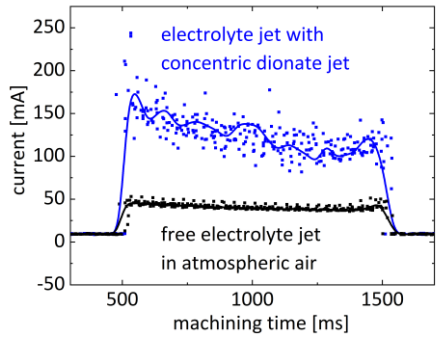

Figure 2. Development of electric current in Jet-ECM over a machining time of 1 s with free electrolyte jet in atmospheric air (black) and with concentric dionate jet (blue). Decreasing trends are caused by ongoing material removal. Significantly higher values with concentric dionate jet indicate a wider current density distribution.

The points refer to a total of 20 experiments from two experimental series, ten of each carried out with and without concentric dionate jet. One exemplary spline was added for one experiment of each of the two series to highlight the current development over machining time.

With free jet of electrolyte surrounded by atmospheric air (black-coloured points) maxima of approximately (40…50) mA were measured in the beginning of the removal processes characterised by the rising current at machining times around 500 s, which corresponds to previous machining experiments considering the lower electrolyte conductivity [11]. A decreasing trend to approximately 10 % lower values until the end of the machining processes is observed, which is caused by the ongoing removal leading to a continuous increase in working gap.

Applying a concentric dionate jet (blue-coloured points) leads to an increase to significantly higher average values between 140 mA and 250 mA with decreasing trend over machining time, as highlighted by the blue-coloured spline. The higher values indicate a significantly wider distribution of current density over the workpiece surface, provided that the shape of the non-diluted, concentric electrolyte jet remains comparable to the free electrolyte jet, and significant dilution effects mainly appear in the surrounding regions of the electrolyte film. The

comparatively large, oscillating deviations were caused by pulsations of the dionate supplying pump.

Top view microscope images of the removal results were captured with a Keyence VK-9700 UV-confocal laser scanning microscope as shown in figure 3.

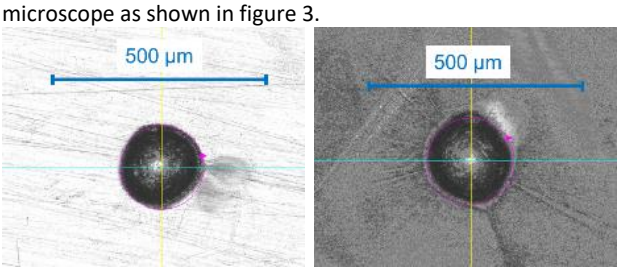

(a) (b)

Figure 3. Top view microscope images of the removals and surrounding areas after Jet-ECM with free electrolyte jet in atmospheric air (left) and with concentric dionate jet (right). No stray removal is cognizable after Jet-ECM with free electrolyte jet, while certain stray removal effects appear when applying a concentric dionate jet.

Both machining experiments led to qualitatively comparable, round-shaped removals caused by the circular cross-sectional shape of the electrolyte jet. From the left-hand microscope image, no stray removal is cognizable after machining with free electrolyte jet, since the initial surface with linear marks from the preparative grinding process remains unchanged. However, certain stray removal on the surrounding surface is cognizable when applying concentric dionate jet, as shown on the right-hand image. Cross-sectional profiles were extracted at the positions marked by the light-blue coloured, horizontal lines. The comparative results are presented in figure 4.

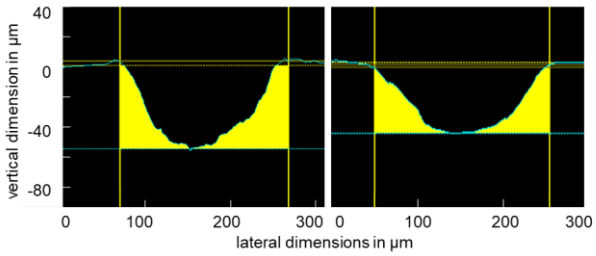

Figure 4. Comparative cross-sectional profiles of the removals after Jet-ECM with free electrolyte jet in atmospheric air (left) and with concentric dionate jet (right). No measurable stray removal with concentric dionate jet indicates only low current density values on the surrounding surface.

The removal realized with free electrolyte jet shown on the left-hand profile has a width of 198 µm with respect to the initial surface at an ordinate value of approximately 100 µm. This is approximately twice the nozzle diameter and corresponds to a value expected from previous experiments. According to the results before, no secondary removal is recognized in the cross-sectional shape. The measured removal depth amounts to 57 µm.

Even if significant stray removal effects were detected before, the comparative analysis of the shape dissolved with concentric dionate jet on the right-hand profile only results in a width of 205 µm. This means hardly a considerable widening by the obviously wider distribution of current density and indicates only low current density values on the surrounding surface, which are expected to be in passivation range when applying a passivating electrolyte. The removal was reduced to 49 µm. Provided a spherical segment-shaped removal, the slight widening and reduced depth results in approximately 10 % reduction of dissolved volume.

4. Results of anodization experiments with electrolyte jet

Current transients of the anodization experiments are presented in figure 5. The points represent the measured values. Straight lines are drawn to connect the measured values to indicate the current pulses for easier retraceability. A representative time slot from 100.00 s to 100.07 s was chosen to assure visible comparison. Low current amplitudes of approximately (0.8 … 1.3) mA are detected, which is due to high electric resistance of the anodic oxide and the confinement of the current flow to restricted areas addressed by the jets.

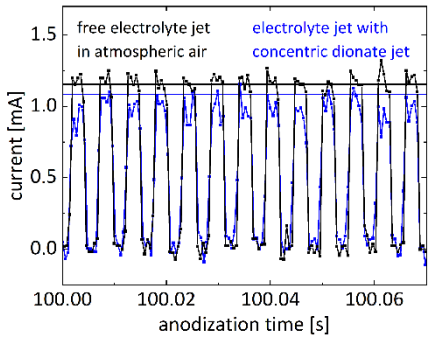

Figure 5. Transients of electric current in anodization experiments over a time section of 0.07 s with free electrolyte jet in atmospheric air (black) and with concentric dionate jet (blue). Approximated amplitudes with concentric dionate jet are slightly lower compared to the free jet.

The horizontal lines represent the calculated 80th percentiles of the measured values. Each was calculated over an anodization time of approximately 2 min to indicate the approximated amplitudes of electric current. With free electrolyte jet (black) an approximated amplitude of 1.15 mA was calculated, while with concentric dionate jet (blue) the approximated amplitude was 1.08 mA. Hence, slightly lower values were determined with concentric dionate jet.

The top view images in figure 6 captured with a Keyence VK-9700 laser scanning microscope show the oxidized areas.

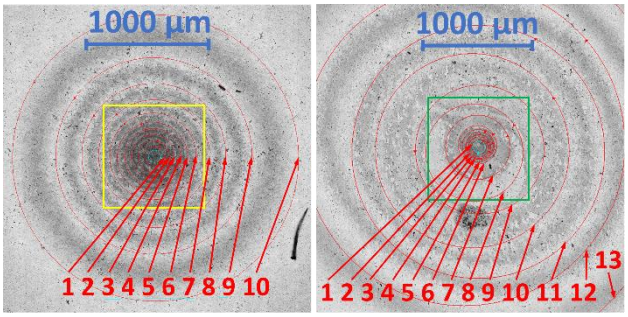

Figure 6. Top view laser scanning images of the anodic oxides realized with free electrolyte jet (left) and with concentric dionate jet (right). The wider distribution and a stronger concentration of interference rings indicating an increased oxide thickness in the centre are cognizable with concentric dionate jet.

The microscope images were captured with an ultraviolet laser light and reveal specific interference rings. Considering the monochromatic laser light with a wavelength λ of 0.408 µm, the thickness of the anodic oxides z_{Ox} was calculated by Bragg's equation (1).

$$z_{Ox} = \frac{i \cdot \lambda}{2 \cdot \sin\alpha \cdot n}. \quad (1)$$

Here, n is the refractive index of the anodic oxide and amounts to 1.68 [14]. The incidence angle of the laser α was 90°. The number of interference rings i was counted from the centre of the anodic oxides outwards as highlighted by the red-coloured rings and the respective numbering.

As can be seen on the left-hand image, circular, concentric interference rings were realized with free electrolyte jet. Ten rings were counted in the analyzed image with an expansion of $X \times Y = 2500 \times 2500\ \mu m^2$. This means an increase in oxide thickness of approximately 1.21 µm from the outer region to the center. The diameter of the outer ring, which was calculated from the measured circumferential length, is assessed to 2318 µm. The inner ring has diameter of 168 µm.

The interference rings shown on the right-hand image, which were detected after anodization with concentric dionate jet, show a slight oval-shaped deviation compared to the circular measuring rings caused by a preferred flow direction of the dionate jet. The diameter of the outer measuring ring is larger and exhibits 3313 µm. 13 interference rings were counted within the analyzed image of the same expansion as before. This represents a larger oxide thickness increase of 1.58 µm. It is assumed that the electrolyte film was successfully diluted by the concentric dionate jet and led to a stronger concentration of electric charge exchange at the impinging electrolyte jet.

The images in figure 7 show detailed views of the respective yellow-coloured and green-coloured rectangles in figure 6. Light blue circles in the centre indicate the outlet diameter of the electrolyte jet.

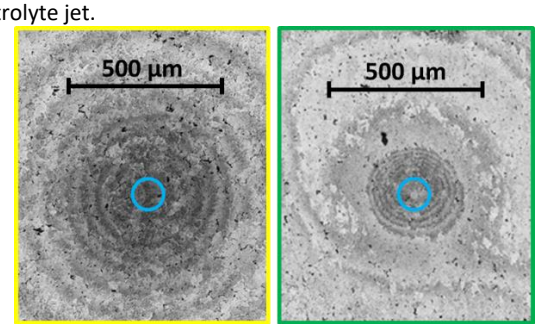

Figure 7. Detailed images of the anodic oxides realized with free electrolyte jet (yellow, left) and with concentric dionate jet (green, right). The stronger concentration of the inner interference rings with concentric dionate jet indicate a narrower transition zone between the outer and inner anodic oxide layer.

While with free electrolyte jet (left), single interference rings can be separated quite well, a strong concentration of interference rings is recognized in the centre of the concentric dionate jet (right). This effect was detected for a lateral expansion of approximately 300 µm, which corresponds to the three-fold of the outlet diameter of the electrolyte jet. An inner ring with a minimal diameter of 122 µm was measured, however, the lateral distance between the single rings decreases in the centre to values below detectable resolution.

Hence, even stronger oxide thickness increase is expected there. Moreover, the inner interference rings in the right-hand image are concentrated to a significantly smaller diameter, which indicates a significantly narrower transition zone between the outer oxide with shallow thickness and the inner oxide with larger thickness. Thus, more massive barrier layer formation and reduced redissolution effects are expected to be realized in the outer regions by the electrolyte film dilution leading to more neutral pH compared to the free electrolyte jet arrangement.

5. Summary

Jet-ECM experiments were carried out with free electrolyte jet surrounded by atmospheric air and with concentric jet of dionate. A significant increase in electric current flow as well as surficial stray removal was detected with concentric dionate jet, which indicates a wider distribution of current density.

Anodization experiments result in very low electric current flow due to the high electric resistance of the anodic oxide and the confinement of the current flow by the jets. The comparative results indicate that electric current flow on the outer surfaces causes widely distributed oxide formation. While with free electrolyte jet interference rings with a maximal diameter of approximately 23-fold of the electrolyte outlet diameter were measured, up to 33-fold of the electrolyte outlet diameter was affected with concentric dionate jet. However, the concentric dionate jet offers formation of locally increased anodic oxide thickness with sharper contoured shape in the centre at a 3-fold of the electrolyte outlet diameter.

6. Conclusions

The main conclusions are the following:

- The comparable removal diameter in Jet-ECM and only slight decrease in dissolved volume indicate only a slight reduction of current density below the nozzle's centre and proves only negligible influence on the impinging jet by the concentric dionate jet.
- No detected secondary removal indicates only low current densities on the surrounding workpiece surface with values in passivation range of passivating electrolytes.
- For surfacial anodic oxidation with the aim to create well-defined, localized structures, the significantly narrower transition zone between the outer shallow layer and the inner thicker layer appears promising.
- It is assumed that the electrolyte film dilution leading to reduced electric conductivity of the electrolyte results in a stronger concentration of electric charge exchange in the near of the impinging jet.
- The dilution of the electrolyte film might result in more massive barrier layer formation and in reduced redissolution effects due to more neutral pH.

Acknowledgment

The researches presented in this study were funded by the Deutsche Forschungsgemeinschaft (DFG, German Research Foundation) – Project number 280132256.

References

[1] Wielage B, Alisch G, Lampke T, Nickel D 2008 *Key Eng. Mater.* **384** 263–281
[2] Schneider M, Fürbeth W 2022 *Mater. Corros.* **73** 1752–1765
[3] Wragg D A, Davies D P, Jenkins S L 2022 *International Journal of Fatigue* **163**
[4] Attolico MA, Casavola C, Moramarco V, Renna G, Furfari D, Busse DO 2022 *Fatigue Fract Eng Mater Struct.* **45** 3716 - 3730
[5] Berndt L, Hartwig A, Kleemeier M, Krieger A, Thiel K, Burchardt M 2016 *Surf. Interface Anal.* **48** 926–933
[6] Vanek D 2010 *Met. Finish.* **108** 25–32
[7] Berndt L, Hartwig A, Kleemeier M, Krieger A, Thiel K, Burchardt M 2016 *Surf. Interface Anal.* **48** 926–933
[8] Rose A, Palani S, Legg K, Kibble V 2019 *DoD-Allied Nations Technical Corrosion Conference*
[9] Siket C M, Mardare A I, Kaltenbrunner M, Bauer S, Hassel A W 2013 *Electrochimica Acta* **113** 755–761
[10] Nickel D, Dietrich D, Morgenstern R, Scharf I, Podlesak H, Lampke T 2016 *Adv. Mater. Sci. Eng* **2016**
[11] Hackert-Oschätzchen M, Meichsner G, Zinecker M, Martin A, Schubert A 2012 *Precision Engineering* **36** 612-619
[12] Morgenstern R, Martin A, Lehnert N, Scharf I, Hackert-Oschätzchen M, Schubert A, Lampke T 2019 *IOP Conference Series: Materials Science and Engineering* **480**
[13] Kuhn D, Martin A, Eckart C, Sieber M, Hackert-Oschätzchen M, Lampke T, Schubert A 2017 *IOP Conference Series: Materials Science and Engineering* **181**
[14] Zeković L D, Urošević V V, Jovanić B R 1986 *Thin Solid Films* **139** 109–113